

Figure S1. Schematic representation of the Htt locus representing the different lines used in this study as well as the relative location and direction of the neo cassette and other locus elements.

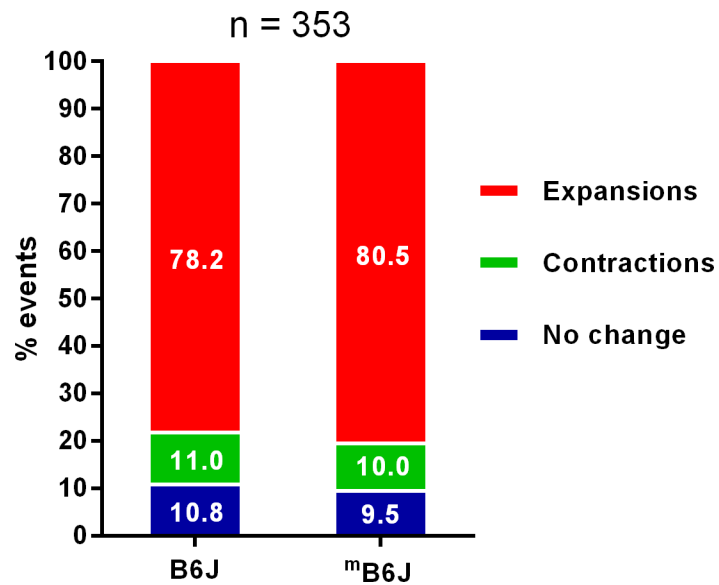


Figure S2. Validation of the frequency modeling methodology for comparison of intergenerational instability across different datasets. Left bar represents the frequencies observed within 50% of the B6J dataset (n=353), while the right bar represents the same dataset with frequencies modeled based on the remaining 50% (n=354) which was used as the reference dataset. No significant differences were observed.

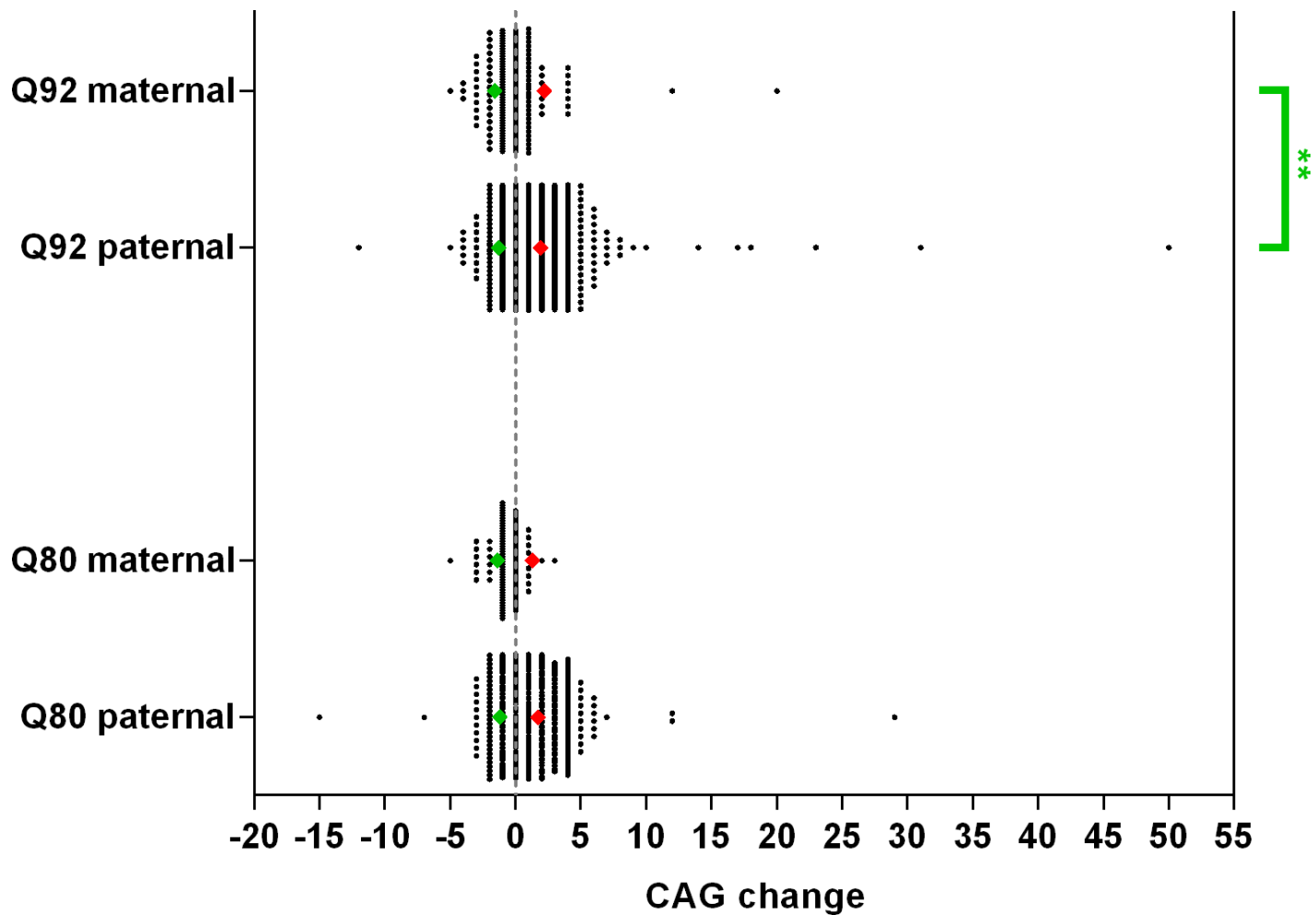


Figure S3. Magnitude of changes in paternal and maternal transmissions (Htt^{Q80} and Htt^{Q92}) in JAX's transmission data. Representation of CAG change for all maternal and paternal transmissions observed (dotted, black), in the Htt^{Q80} and Htt^{Q92} lines, as well as mean expansion (diamonds, red) and mean contraction (diamonds, green) values (see also Table 2 and Table 3).

**p<0.01

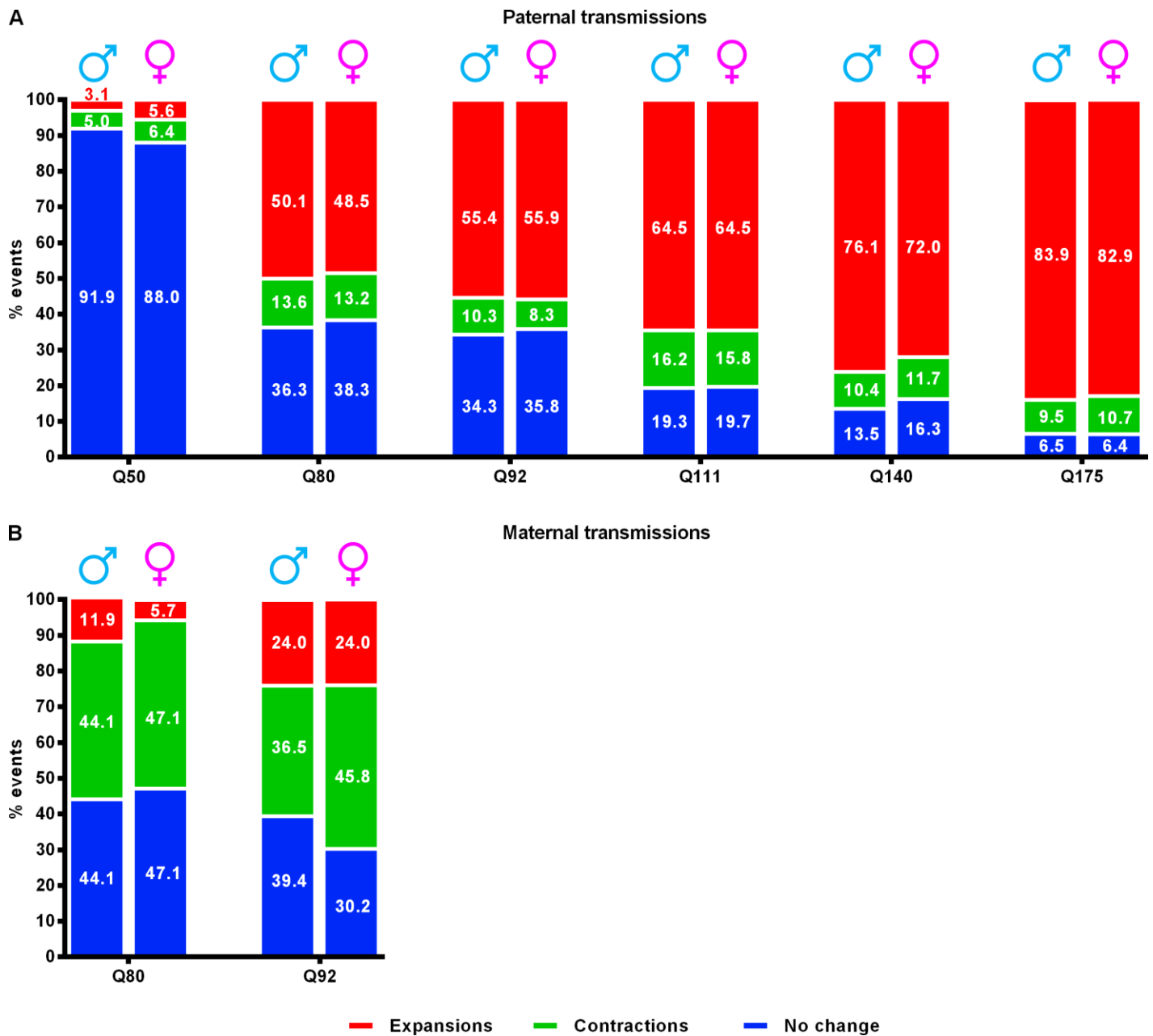
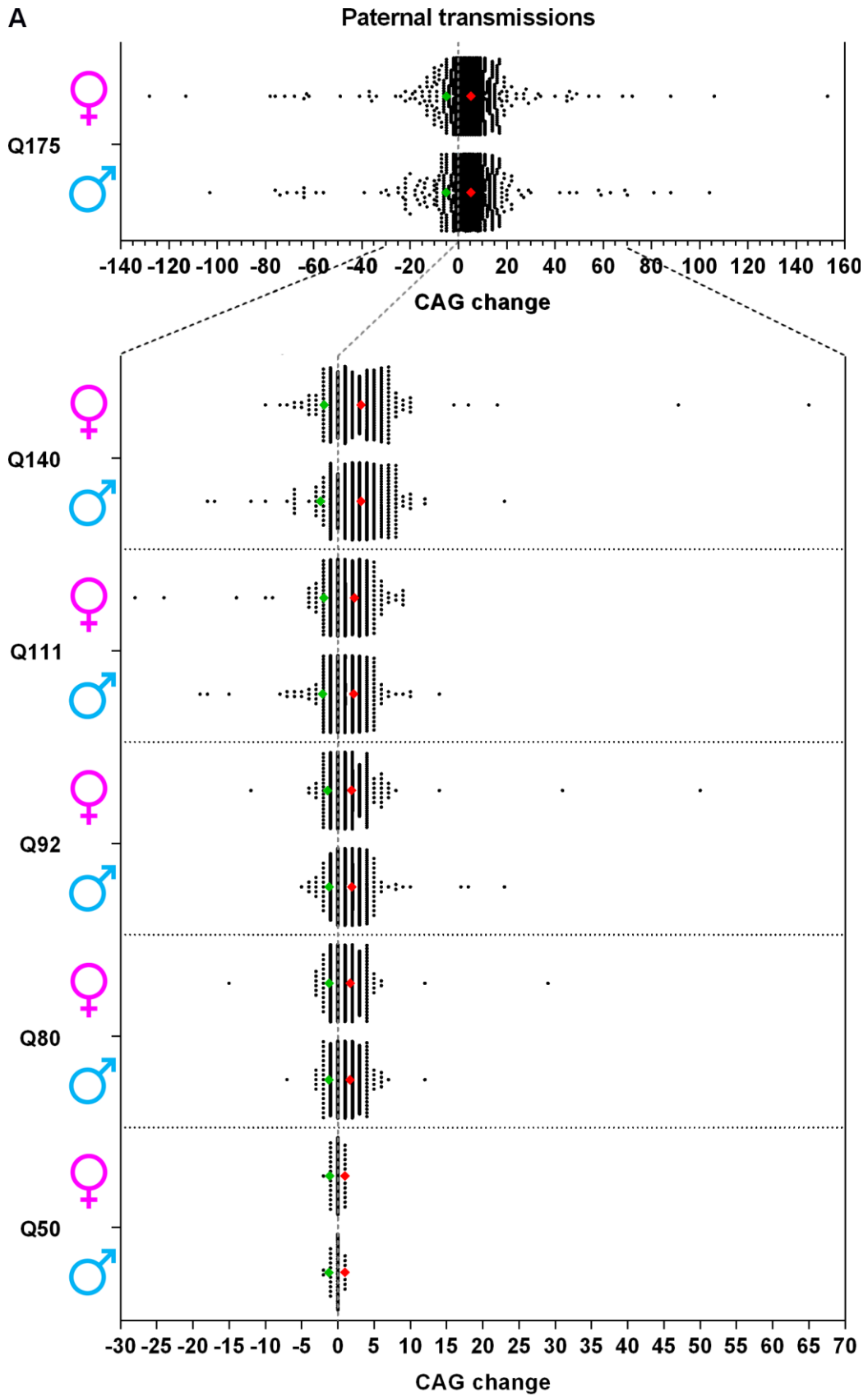


Figure S4. Relative frequency of stable and unstable transmissions by offspring sex in the JAX *Htt* CAG knock-in dataset. Breakdown of transmission frequency by expansions (red), contractions (green) and stable transmissions (blue) separated by offspring sex among paternal (A) and maternal (B) transmissions.



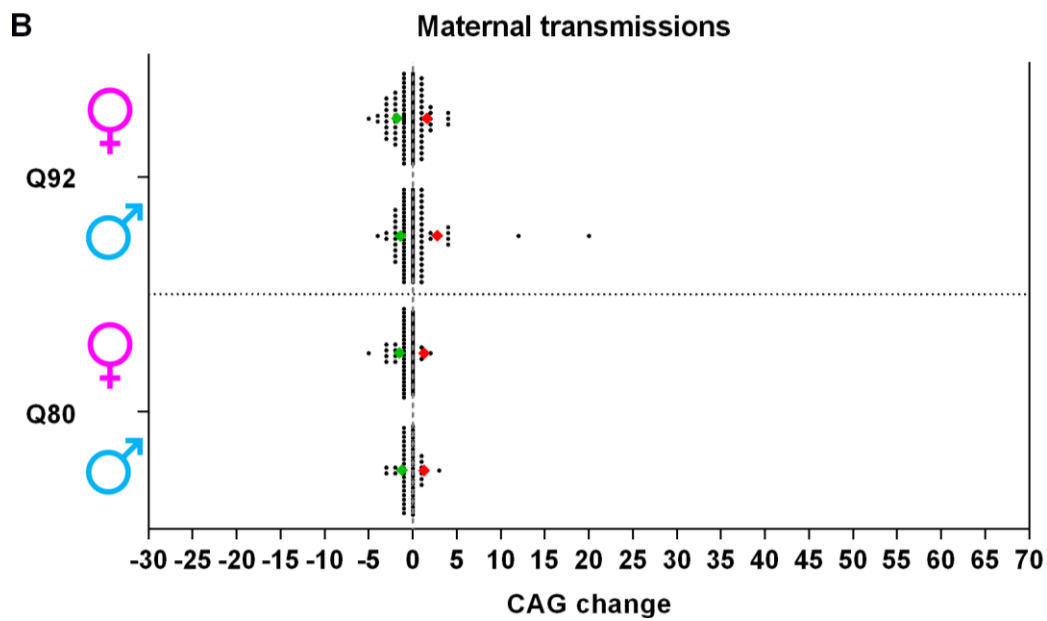


Figure S5. Magnitude of changes segregated by offspring sex in paternal and maternal transmissions in JAX's transmission data. Representation of CAG changes for all paternal (A) and maternal (B) transmissions observed (dotted, black) in the available lines, as well as mean expansions (diamonds, red) and mean contractions (diamonds, green).

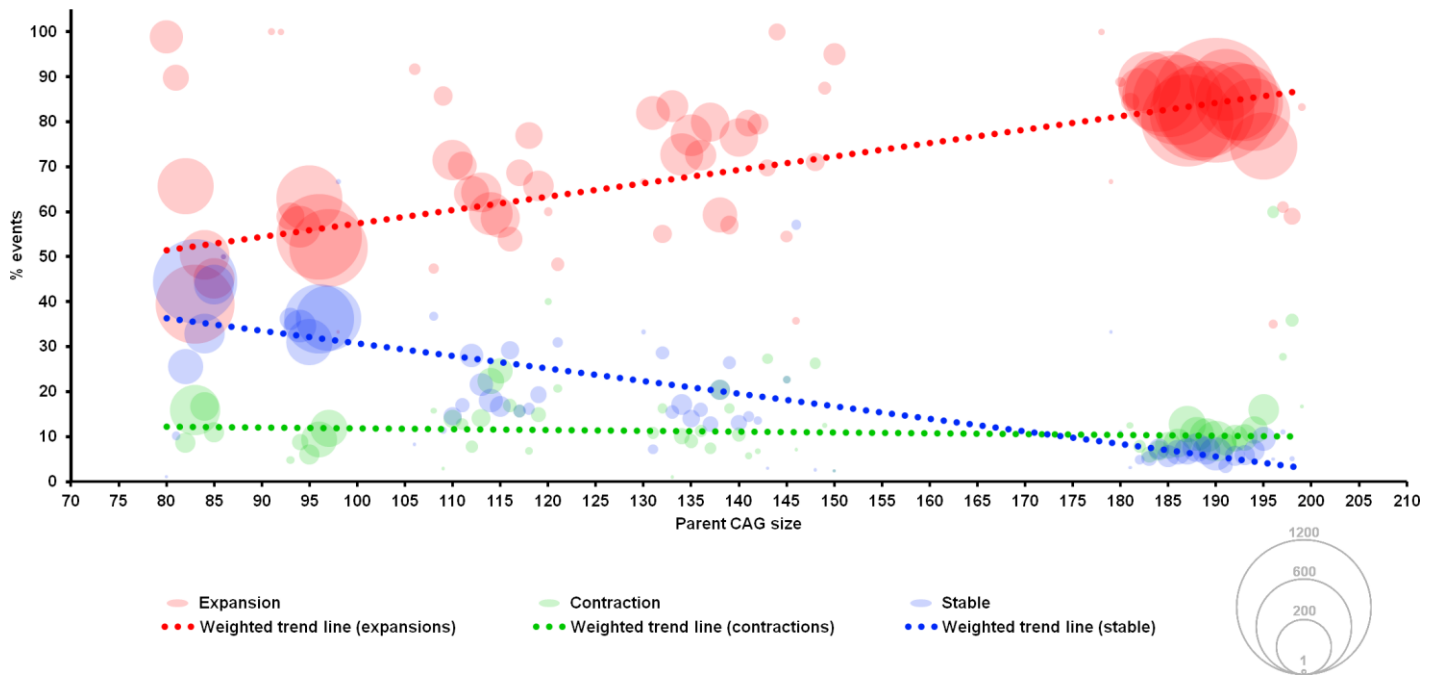


Figure S6. Relative frequency of stable and unstable (expansions, contractions) transmissions by paternal CAG size in JAX's dataset. Breakdown of transmission frequency by expansions, contractions and stable transmissions using paternal CAG size as a continuous variable. Trend lines weighed by the total number of observed transmissions for each parental CAG length are represented as dotted lines. Bubble size is proportional to the total number of observed events. Events with null frequency (N=0) are considered for trend line weighing but are not depicted as bubbles.

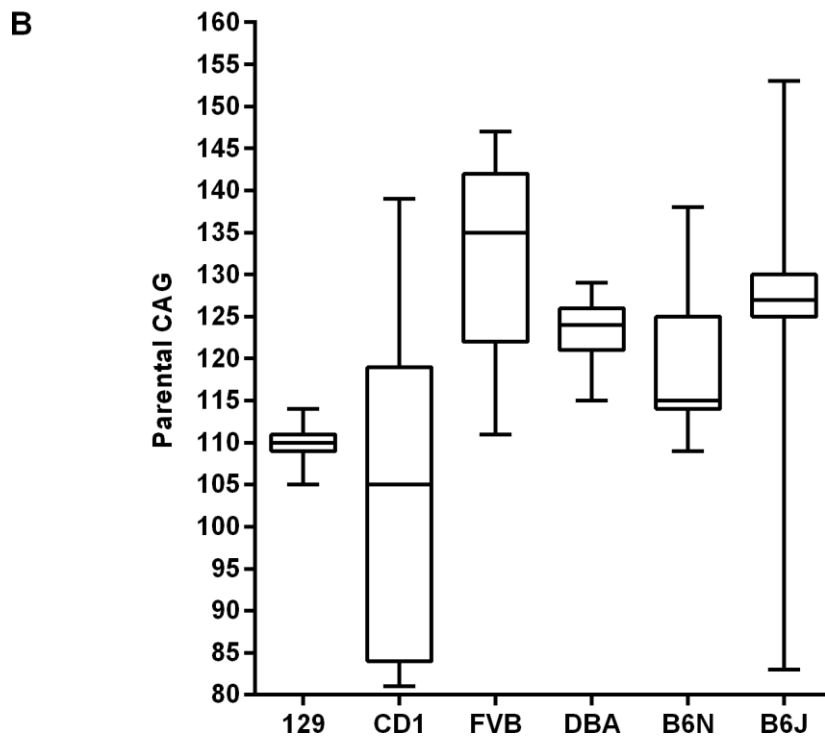
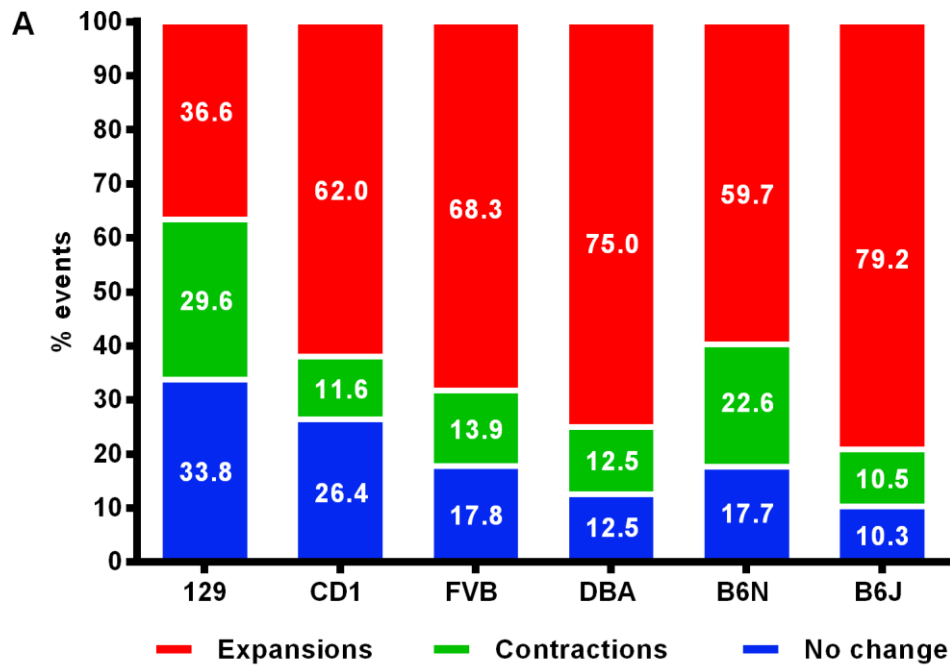


Figure S7. Frequency of changes and paternal CAG sizes across the six genetic backgrounds.

(A) Frequency of expansions, contractions and stable transmissions across different strains in the CHGR breeding dataset (B) Parental CAG range among the six strains (boxes encompass 50% of total transmissions, whiskers represent minimum to maximum size).

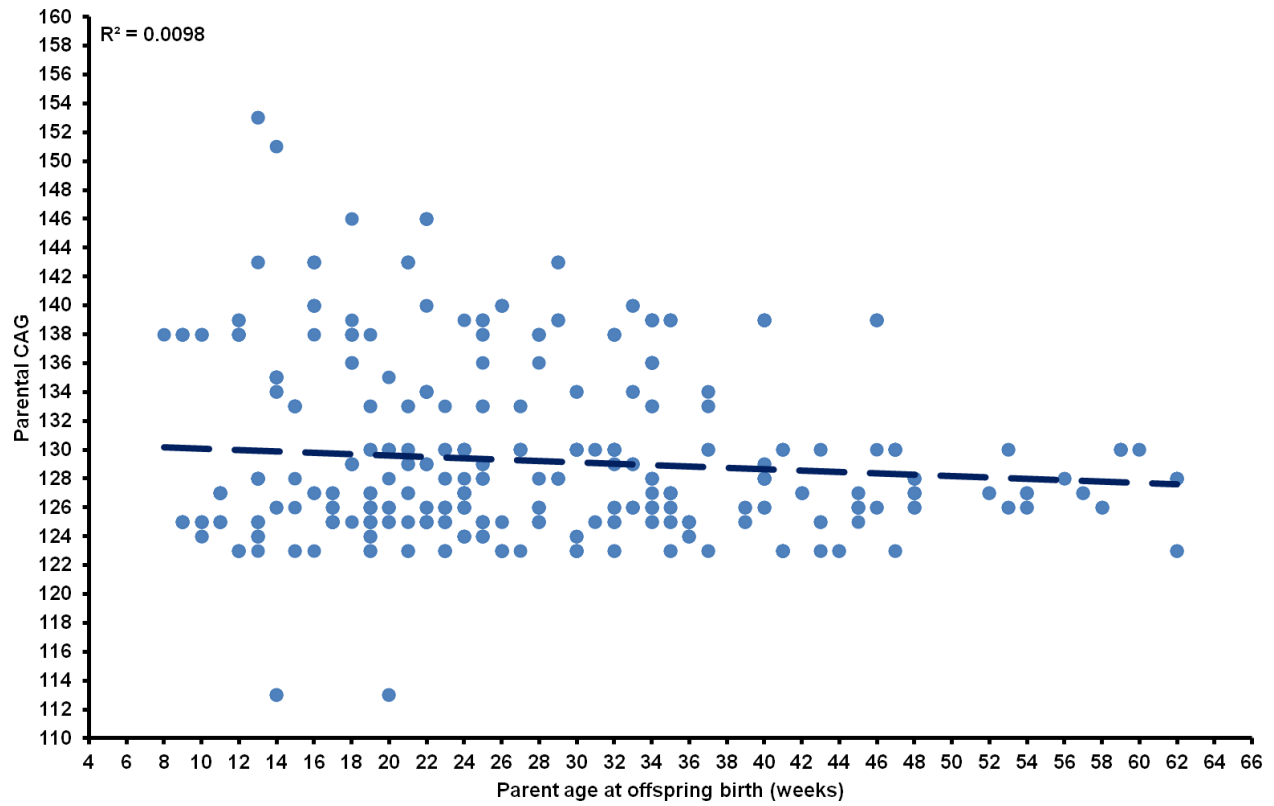


Figure S8. Distribution of parental CAG repeat size across paternal age at birth in the B6J.*Htt*^{Q111} mice (113-153 CAGs; N=690 transmissions) in CHGR's breeding dataset.

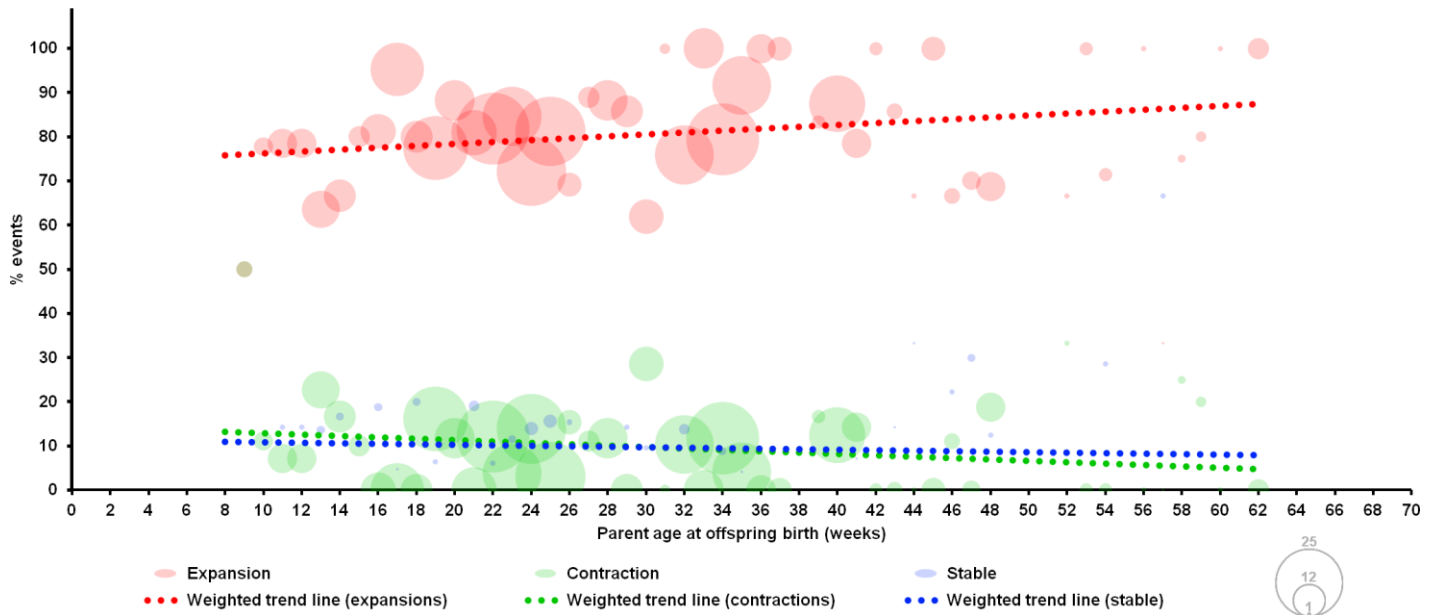


Figure S9. Frequency of changes by paternal age at offspring birth (B6J background, CHGR dataset). Trend lines weighed by the total number of observed transmissions for each parental age are represented as dotted lines. Bubble size is proportional to the total number of observed events. Events with null frequency (N=0) are considered for trend line weighing but are not depicted as bubbles.

A

Paternal transmissions

Line	to male offspring									to female offspring						
	Total	Stable	Contractions			Expansions			Total	Stable	Contractions			Expansions		
	N	N (%)	N (%)	Max.	Mean	N (%)	Max.	Mean	N	N (%)	N (%)	Max.	Mean	N (%)	Max.	Mean
Q50	260	239 (91.9)	13 (5.0)	2	1.2	8 (3.1)	1	1.0	251	221 (88.0)	16 (6.4)	2	1.1	14 (5.6)	1	1.0
Q80	1184	430 (36.3)	141 (13.6)	7	1.2	593 (50.1)	12	1.7	1281	491 (38.3)	169 (13.2)	15	1.2	621 (48.5)	29	1.7
Q92	1427	489 (34.3)	147 (10.3)	5	1.2	791 (55.4)	23	1.9	1456	521 (35.8)	121 (8.3)	12	1.4	814 (55.9)	50	1.9
Q111	772	149 (19.3)	125 (16.2)	19	2.1	498 (64.5)	14	2.2	778	153 (19.7)	123 (15.8)	28	1.9	502 (64.5)	9	2.3
Q140	779	105 (13.5)	81 (10.4)	18	2.4	593 (76.1)	23	3.2	779	127 (16.3)	91 (11.7)	10	1.9	561 (72.0)	65	3.2
Q175	4719	309 (6.5)	450 (9.5)	103	5.1	3960 (83.9)	104	5.2	4453	283 (6.4)	477 (10.7)	128	5.0	3693 (82.9)	153	5.2

N, number

B

Maternal transmissions

Line	to male offspring									to female offspring						
	Total	Stable	Contractions			Expansions			Total	Stable	Contractions			Expansions		
	N	N (%)	N (%)	Max.	Mean	N (%)	Max.	Mean	N	N (%)	N (%)	Max.	Mean	N (%)	Max.	Mean
Q80	59	26 (44.1)	29 (44.1)	3	1.2	7 (11.9)	3	1.3	70	33 (47.1)	33 (47.1)	5	1.5	4 (5.7)	2	1.3
Q92	104	41 (39.4)	38 (36.5)	4	1.4	25 (24.0)	20	2.8	98	29 (30.2)	44 (45.8)	5	1.8	23 (24.0)	4	1.6

N, number

Table S1. Paternal and maternal transmission data for the different lines segregated by offspring sex in JAX's breeding data.

		χ^2 tests of independence regarding offspring gender		
Line	Transmission	χ^2	df	p-value
<i>Htt</i> ^{Q50}	Paternal	2.493	2	0.287
<i>Htt</i> ^{Q80}	Paternal	1.065	2	0.587
	Maternal	1.553	2	0.460
<i>Htt</i> ^{Q92}	Paternal	3.574	2	0.167
	Maternal	2.263	2	0.323
<i>Htt</i> ^{Q111}	Paternal	0.062	2	0.970
<i>Htt</i> ^{Q140}	Paternal	3.555	2	0.169
<i>Htt</i> ^{Q175}	Paternal	3.532	2	0.171

Table S2. χ^2 and p-values for offspring sex effect on the relative frequencies of contractions, expansions and stable alleles in the JAX *Htt* CAG knock-in dataset.

Line	Paternal CAG			Transmissions							
				N	Stable	Contractions		Expansions			
	Min.	Max.	Mean		N (%)	N (%)	Max.	Mean	N (%)	Max.	Mean
CD1 ^{neo-}	81	139	105.7	439	116 (26.4)	51 (11.6)	8	1.7	272 (62.0)	12	1.8
CD1 ^{neo+}	113	135	122.6	152	42 (27.6)	18 (11.8)	2	1.4	92 (60.5)	8	2.1
adj CD1 ^{neo-}	114	134	121.5	170	35 (20.6)	14 (8.2)	6	1.6	121 (71.2)	12	2.1
Q175 ^{neo+}	178	199	188.9	9172	592 (6.5)	927 (10.1)	128	5.1	7653 (83.4)	153	5.2
Q175 ^{neo-}	180	192	187.1	256	9 (3.5)	14 (5.5)	88	9.1	233 (91.0)	30	5.7
adj Q175 ^{neo+}	180	192	187.8	7541	473 (6.3)	706 (9.4)	128	5.4	6362 (84.4)	153	5.2

Table S3. Characteristics of paternal CAG intervals and transmission frequency and magnitude in the *neo+*, *neo-* and adjusted datasets.